Letter | Editors' Suggestion

Realization of a tunable surface Dirac gap in Sb-doped $MnBi_2Te_4$

Xiao-Ming Ma,[1,*] Yufei Zhao,[1,*] Ke Zhang,[2,*] Shiv Kumar,[3,*] Ruie Lu,[1] Jiayu Li,[1] Qiushi Yao,[1] Jifeng Shao,[1] Fuchen Hou,[1] Xuefeng Wu,[1] Meng Zeng,[1] Yu-Jie Hao,[1] Zhanyang Hao,[1] Yuan Wang,[1] Xiang-Rui Liu,[1] Huiwen Shen,[1] Hongyi Sun,[1] Jiawei Mei,[1] Koji Miyamoto,[3] Taichi Okuda,[3] Masashi Arita,[3] Eike F. Schwier,[3] Kenya Shimada,[3] Ke Deng,[1] Cai Liu,[1] Junhao Lin,[1] Yue Zhao,[1] Chaoyu Chen,[1,†] Qihang Liu,[1,4,‡] and Chang Liu[1,§]

[1]*Shenzhen Institute for Quantum Science and Engineering (SIQSE) and Department of Physics, Southern University of Science and Technology (SUSTech), Shenzhen, Guangdong 518055, China*

[2]*Department of Physical Science, Graduate School of Science, Hiroshima University, 2-313 Kagamiyama, Higashi-Hiroshima 739-0046, Japan*

[3]*Hiroshima Synchrotron Radiation Center, Hiroshima University, 2-313 Kagamiyama, Higashi-Hiroshima 739-0046, Japan*

[4]*Guangdong Provincial Key Laboratory for Computational Science and Material Design, Southern University of Science and Technology (SUSTech), Shenzhen, Guangdong 518055, China*

(Received 1 July 2020; revised 19 February 2021; accepted 24 February 2021; published 17 March 2021)

Signatures of both the quantum anomalous Hall effect and axion electrodynamics have been recently observed to exist in thin films of $MnBi_2Te_4$, a stoichiometric antiferromagnetic topological insulator. Direct evidence of the bulk topological magnetoelectric response in an axion insulator requires an energy gap at its topological surface state (TSS). However, independent spectroscopic experiments revealed that such a surface gap is much smaller than previously thought. Here we utilize angle resolved photoemission spectroscopy and density functional theory calculations to demonstrate that a sizable TSS gap unexpectedly exists in Sb-doped $MnBi_2Te_4$ where the bulk system remains topologically nontrivial. This gap is found to be insensitive to the bulk antiferromagnetic-paramagnetic transition, while it enlarges along with increasing Sb concentration, enabling simultaneous tunability of the Fermi level and the TSS gap size (up to >100 meV). Our work shows that Sb dopants in $MnBi_2Te_4$ can not only control the Fermi level but also induce a tunable surface gap, providing a potential platform to observe the key features of the high-temperature axion-insulator phase.

DOI: 10.1103/PhysRevB.103.L121112

Magnetic topological insulators (MTIs) are condensed matter systems that possess long-range magnetic order but remain topologically nontrivial [1–3]. Compared to nonmagnetic TIs whose topological surface states (TSSs) manifest a gapless Dirac cone that is protected by time reversal symmetry ($\mathcal{T}$), the TSSs of MTIs could open an energy gap if out-of-plane ferromagnetic (FM) order exists at the surface [4]. The presence of this gap in MTIs is of central importance to reveal the bulk topological magnetoelectric response in a so-called "axion insulator", as each of these gapped surfaces hosts an anomalous Hall conductivity (AHC) that is quantized to a half of e^2/h [5–7]. Albeit much less explored than the quantum anomalous Hall state [8–10], axion insulators shed light on the fundamental understanding of topological insulators as bulk magnetoelectrics [2,11], and are potentially practical even in the astronomical search for the dark axions, quasiparticle candidates of the long-sought nonbaryonic dark matter [12].

The newly discovered van der Waals magnetic compounds $(MnBi_2Te_4)(Bi_2Te_3)_n$ $(n = 0, 1, 2, ...)$ are thus far the only stoichiometric material system that enables both the quantum anomalous Hall and the axion insulator states [13–19], whose Dirac surface state is first detected by angle-resolved photoemission spectroscopy (ARPES) [20]. The ground-state magnetic orders of the $n < 2$ compounds are found to be *A*-type antiferromagnetic (AFM), with out-of-plane moments coming from the central Mn planes of the septuple-layer (SL) building blocks [16,21–27]. Along with strong band inversion, these compounds are predicted to be three-dimensional AFM TIs and strong candidates of axion insulators with TSS gaps at their natural cleaving planes [4,13,28]. Intriguingly, ARPES and scanning tunneling spectroscopy (STM) measurements uncovered near-vanishing surface state gaps in single crystals of the undoped "parent" compounds [29–37], raising the question of whether the impurities, defects, and possible surface structural and magnetic reconstruction plays a role in realizing the macroscopic quantum phases [29]. Above all, if a surface state gap exists in any of the Mn-Bi-Te family at all is still controversial [29–41].

Antimony is a convenient choice of nonmagnetic atomic dopant in the Bi-based topological materials. In $Bi_2(Se,Te)_3$, Sb is known to effectively introduce holes to the otherwise *n* doped system [42,43]. Meanwhile, it also drives the system towards the topologically trivial side continuously, while maintaining the Dirac cone before the topological phase transition because the $\mathcal{T}$ symmetry is always preserved [44]. Here, we demonstrate via systematic ARPES measurements that the situation in $MnBi_2Te_4$ is fundamentally different. Besides the overall *p*-type doping behavior, a sizable global surface state gap opens in Sb-doped $MnBi_2Te_4$ single crystals. A relatively small concentration of Sb dopants was able to raise the gap

*These authors contributed equally to this work.
†chency@sustech.edu.cn
‡liuqh@sustech.edu.cn
§liuc@sustech.edu.cn

size up to >100 meV. This gap remains immune from the AFM ground state to the high temperature paramagnetic (PM) state, while it increases monotonically with the density of p dopants. Therefore, Sb dosage enables convenient control of the surface state gap in the AFM TI $MnBi_2Te_4$ within a wide range. Based on the modern theory of doping and alloying implemented to density functional theory (DFT) calculations, we identified the signature of the electronic structure during the magnetic phase transition, and confirmed the nontrivial topological nature of the bulk within the doping range studied. Possible origins of the anomalous surface gap are also discussed.

Physical and topological properties of Sb-doped $MnBi_2Te_4$ $\{Mn_{1-\alpha}(Bi_{1-x}Sb_x)_2Te_{4-\beta}$, See Section S2 in Ref. [45]$\}$is a subject of intense recent study [65–69]. Our successful doping of Sb into $MnBi_2Te_4$ is first confirmed by atomic energy dispersive x-ray spectrum (EDX) mapping on a set of samples with nominal doping levels $0 \leqslant x_{\text{nominal}} \leqslant 0.1$ (Section S2 [45]). Together with cross-sectional scanning transmission electron microscopy (STEM) (Section S3 [45]), we found reasonably uniform distribution of Sb dopants over a microscopic region but considerable sample-to-sample variation of doping concentration. Topographic images, obtained by scanning tunneling microscopy, reveal no trace of surface atomic reconstruction and surface lattice constant change (Section S4 [45]). Variation of carrier concentration is also found via Hall measurements between growth batches with different nominal doping, as well as via different samples in the same growth batch (Section S5 [45]). We then distinguish the bulk and surface dispersion and demonstrate the existence of the surface state gap in Sb-doped $MnBi_2Te_4$ via systematic ARPES measurements. Figure 1 shows our ARPES data taken on a typical sample with $x_{\text{nominal}} = 0.075$ at $T = 10$ K (below $T_N \sim 23$ K). Figures 1(a)–1(c) present the raw and second derivative ARPES k-E maps along the $\bar{\Gamma}$-$\bar{M}$ high symmetry direction taken under three representative photon energies, corresponding to two consecutive bulk Γ points and a bulk Z point in between. Great care was taken in these measurements to ensure that the $\bar{\Gamma}$ points are reached very accurately (with uncertainty less than 0.2° for all photon energies), so that the sizes of the global gaps are measured precisely. A clear, sizable energy gap is observed with an identical value at the crossing point of the otherwise linear bands in three different photon energies. This is in drastic contrast to the case of undoped $MnBi_2Te_4$, where the gap is close to diminishing at the Dirac point (see also Section S6 [45] for the existence of the gap in the k_x-k_y plane). From Fig. 1(d) we found that the gap is a global one, which opens under all photon energies measured, covering more than two out-of-plane Brillouin zones (BZs). There are five visible bands [defined in Fig. 1(b)] near the apparent gap (See Section S7 [45] for details of gap size determination). The bulk nature of the BV band is proven via its strong and periodic k_z dispersive behavior seen in Fig. 1(d). The SV and SC bands, on the other hand, exhibit no discernible dispersion across a k_z range of $\sim 5\pi/c$, endorsing their surface origin. We can therefore unambiguously conclude that the surface state of Sb-doped $MnBi_2Te_4$ is gapped.

In Fig. 2 we examine quantitatively the temperature evolution of the bulk and surface bands from the ARPES data on

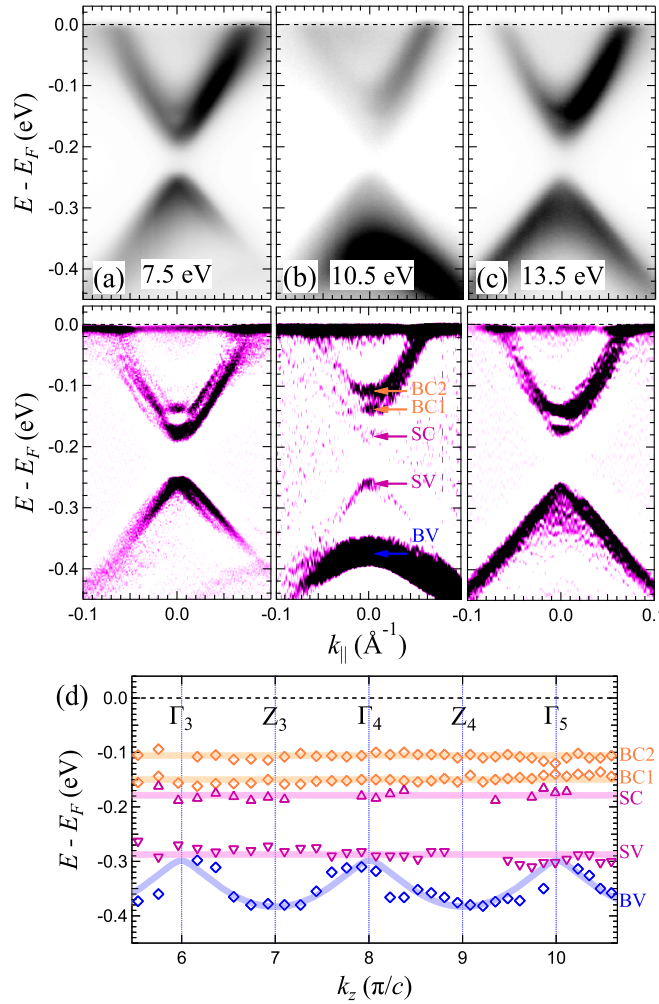

FIG. 1. Presence of the surface state gap in Sb-doped $MnBi_2Te_4$. Data taken on a $x_{\text{nominal}} = 0.075$ sample at $T = 10$ K. (a)–(c) Raw (top) and second derivative (bottom) ARPES k-E maps on three representative photon energies, close to the bulk high-symmetry points (a) Γ_3, (b) Z_3, and (c) Γ_4, respectively. BV: bulk valence band; SV/SC: surface valence/conduction band (bottom/top part of the gapped surface state); BC1/BC2: the two bulk conduction bands seen at $T < T_N$. The persistence of the surface state gap and the evolution of BV is seen clearly. (d) Extraction of k_z dispersion for the bands at $\bar{\Gamma}$. Photon energy ranges from 6.5 to 23 eV, corresponding to $\sim 5.5\pi/c < k_z < \sim 10.6\pi/c$. Colored lines are guides to the eye.

a prototypical Sb-doped sample [Sample S2, $x_{\text{nominal}} = 0.05$, Figs. 2(a)–2(d)], as well as the theoretical AFM and PM electronic structures of bulk $Mn(Bi_{1-x}Sb_x)_2Te_4$ at $x_{\text{cal}} = 0.056$ (1/18) calculated by DFT [Figs. 2(e)–2(h)]. To simulate the electronic structure of Sb doping and the PM phase with randomly distributed local moments, we apply DFT calculations using the Special Quasirandom Structures (SQS) method [70] that takes into account the local disorder effects. To directly compare with the ARPES spectral function, we unfold the resulting band structures obtained from the supercell approach [52,53] to the BZ of the primitive cell. As shown in Figs. 2(e)–2(h), while the slightly doped system for the AFM phase does not change much, the long wavevector spectral density away from E_F for the PM phase looks fuzzy,

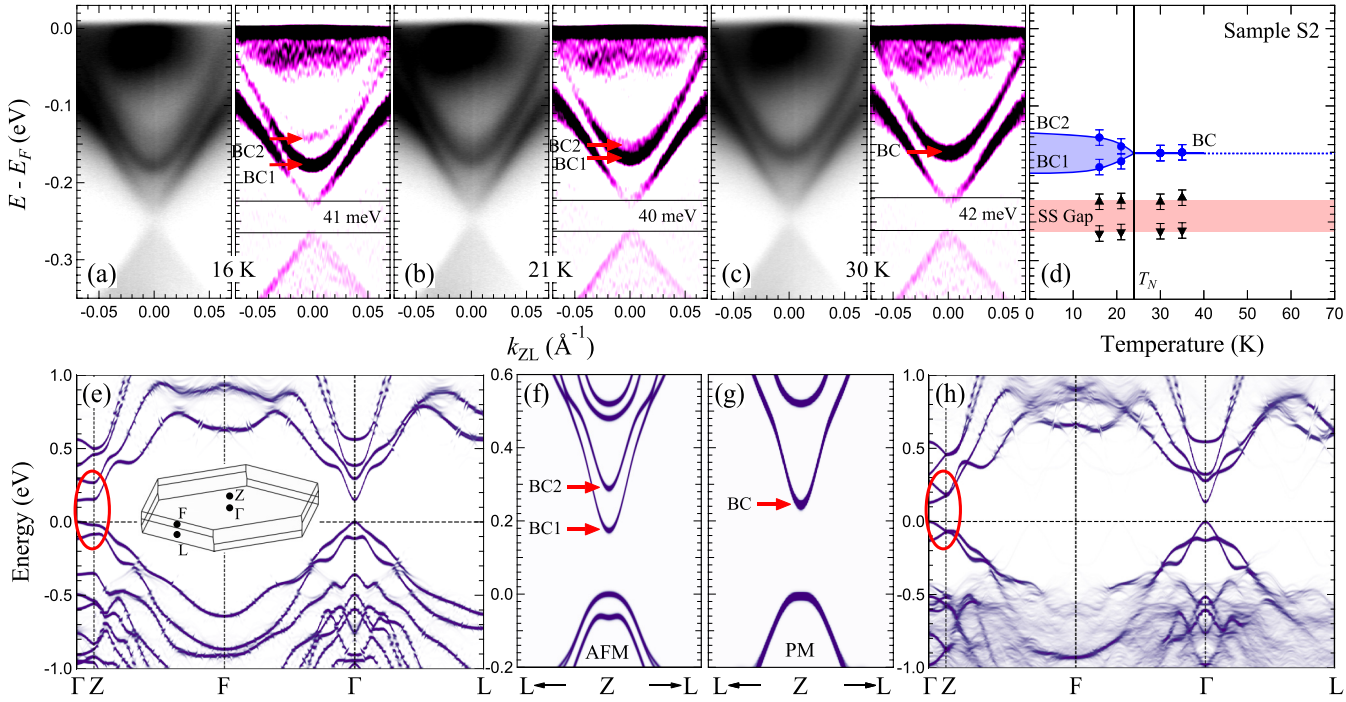

FIG. 2. Temperature independence of the bulk and surface state gap. (a)–(d) Temperature evolution of the bands of Sample S2 ($x_{\text{nominal}} = 0.05$). Data is taken with a 6.36-eV laser ARPES setup [i.e., at $k_z \sim 5\pi/c$ (Z_2)]. (a)–(c) Raw (left) and second derivative (right) ARPES k-E maps taken at three representative temperatures, below and above the bulk AFM-PM transition temperature $T_N \sim 23.5$ K. (d) Summary on the temperature evolution of BC1, BC2, and the surface state (SS) gap. While BC1 and BC2 merges into a single bulk conduction (BC) band around T_N, the SS gap remains essentially unchanged. (e)–(h) Effective band structure (EBS) calculation results for the AFM and PM state electronic structure on a $x = 1/18$ (0.056) system. (e)/(h) Overall band structure of the AFM/PM state. Inset: AFM Brillouin zone with high-symmetry points. Red ellipses highlight the merging of BC1 and BC2 at Z. (f)/(g) Focused band structure of the AFM/PM state along L-Z-L.

informing the extent to which the translational symmetry is retained. The most profound difference of the band dispersion between AFM and PM phases near E_F occurs at the Z point, where the BC1 and BC2 bands merge into a single BC band at the high-temperature PM phase. We note that such "Zeeman-like" band splitting and merging [Figs. 2(f)–2(g)] only happens at the BZ boundary such as the $Z(0, 0, 0.5)$ and $L(0, 0.5, 0.5)$ points. We attribute this phenomenon to the band folding effect due to the doubled primitive cell of the AFM phase with lower translational symmetry compared to the PM phase. Such a spectroscopy signature can be used to monitor the magnetic phase transition. Therefore, we perform ARPES measurements at a photon energy of 6.36 eV, focusing on the bulk Z_2 point ($k_z \sim 5\pi/c$). Indeed, we see in Figs. 2(a)–2(d) that the BC1 and BC2 bands come closer to each other as the temperature rises, merge into a single BC band around $T_N \sim 23.5$ K, and finally keep a constant binding energy for $T > T_N$. Therefore, the band evolution through the AFM-PM magnetic phase transition is unambiguously observed.

Surprisingly, the surface gap on the other hand remains essentially unchanged for all temperatures measured, across T_N from 16 K to 35 K [Fig. 2(d)]. In Fig. S7 [45] we graph the temperature evolution of this gap for two other samples with different x, reproducing again a constant-sized gap up to 150 K. These observations reveal an unexpected fact that the surface state gap of Sb-doped $MnBi_2Te_4$ is insensitive to the change of temperature, regardless of its bulk magnetic phase. Another important feature about the gap is that it increases in samples (or regions) with higher p-type dopants. This behavior is elaborated in Fig. 3 where the sizes of both the SS and the bulk gap are compared at $T > T_N$ [71] for seven samples with different carrier densities, corresponding to $0 \leqslant x_{\text{nominal}} \leqslant 0.1$. Since the actual carrier concentration varies within the same growth batch and even the same sample (Sections S2 and S11 [45]), the doping levels are calibrated using the binding energies at the center of the SS gap (E_c) instead of x_{nominal}. This procedure is justified by the knowledge that Sb atoms are effective p dopants of the system, pushing the Fermi level downward in a rigid band shifting scenario except for the gap region. From Figs. 3(a)–3(e), we see that the gap size increases as E_c increases, from ~12 meV at Sample S1 ($x = 0$, $E_c = -272$ meV) [72] to 122 meV at Sample S5 ($E_c = -156.5$ meV). Local doping variation in a single sample gives different E_c values at different spatial positions, causing a synchronous change of the gap size (Section S11 [45]). Importantly, Fig. 3(f) and Fig. S10 show that the TSS gap and E_c values aligned nicely to a single linear relation. It did not matter if they were measured in different samples or within the same crystal [73].

So far we have demonstrated the presence and the anomalous temperature-doping dependence of a global energy gap in the TSS of Sb-doped $MnBi_2Te_4$. This gap is nearly constant across a wide temperature range, insensitive to the bulk

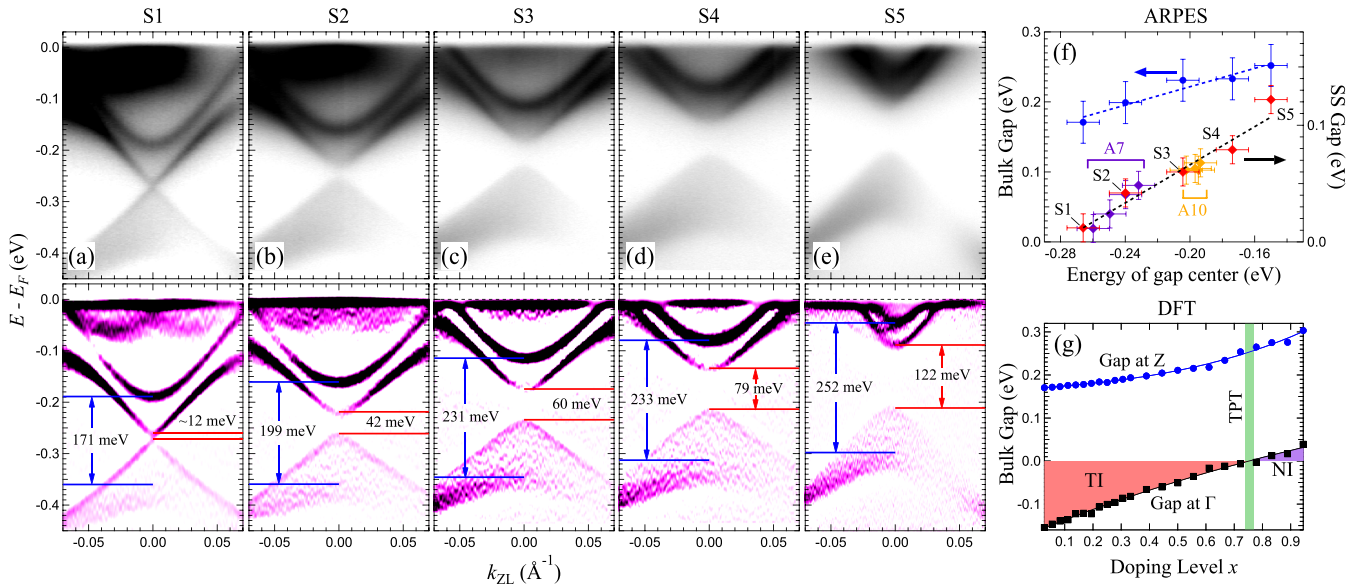

FIG. 3. Carrier concentration dependence of the SS gap and the bulk gap. Data is taken with a 6.36-eV laser ARPES setup at T = 30-35 K (above T_N). (a)–(e) Raw (top) and second derivative (bottom) ARPES k-E maps for five samples with different carrier concentrations ordered by E_c. Red/blue lines: SS/bulk gap. (f) E_c dependence of the bulk gap at Z (blue, left), and the SS gap (black, right). Data taken with Samples A7 and A10 (Section S11 [45]) is also included. (g) Bulk gap at Γ (black) and Z (blue) calculated via supercell approach. Possible errors due to different Sb configuration are within symbol size. Solid lines are polynomial fits. TI: topological insulator; NI: normal insulator; TPT: topological phase transition.

magnetic transition, but enlarges monotonically with increasing p dopants. Before looking into the possible origins of these gapped phases, we first point out that the bulk system remains topologically nontrivial within the doping range studied. Experimentally, we notice that the size of the bulk gap between the BV and the BC bands is increasing with doping at the bulk Z point (Fig. 3), from 171 meV at Sample S1 to 252 meV at Sample S5 (See Section S8 [45] for details of gap size determination), while decreasing with doping at the bulk Γ point (Section S10 [45]). This proves that the bulk system evolves toward the topologically trivial side, but has not yet reached the topological phase transition. Theoretically, our DFT calculations using the SQS method show that the topological phase transition (TPT) in $Mn(Bi_{1-x}Sb_x)_2Te_4$ occurs at a much larger x. Figure 3(g) marks the TPT by displaying the calculated band gap evolution at Γ and Z. Both the growing gap at Z and the decreasing gap at Γ with increasing x is consistent with our ARPES results. The gap at Γ closes at $x_c \simeq 0.75$, where the system undergoes a transition to the normal-insulator state. Similar calculation results using the virtual crystal approximation (VCA) [64] are shown in Section S14 [45], in which x_c is found to be about 0.65. Therefore, for $0 \leqslant x \leqslant 0.1$, the system stays in the topological regime.

We note that the TSS of the $x = 0$ parent compound has a near-vanishing gap that is much smaller than DFT prediction (Figs. 2, 3 and Refs. [29–32]). Although a comprehensive explanation on the intact Dirac cone of $MnBi_2Te_4$ is not reached, these results point to the possibility that the structural and/or magnetic structure on the surface of the system is fundamentally different from that in the bulk [29]. Thus, it is natural to speculate that Sb doping in $MnBi_2Te_4$ suppresses the surface spin reorientation and somehow restore the surface FM, which is supported by the ferrimagnetic state recently found by transport measurements in Sb-doped samples [74]. However, this argument is not consistent with our ARPES results in the PM phase, because a magnetic gap arising from this mechanism is supposed to vanish at $T > T_N$. Similarly, previous work proposed that the Dirac electronic states could couple to the conduction electrons through the Ruderman-Kittel-Kasuya-Yosida (RKKY) exchange interaction among the PM impurities, and thus induce weak ferromagnetism [75]. However, it is uncertain that such a FM state above T_N could quantitatively cause a ∼100 meV gap as found, which inevitably leads to a significantly higher transition temperature at the surface. The residual FM at the surface is supposed to be captured by monitoring the s_z components of the TSS from the spin-ARPES measurements [56]. We performed such measurements on an undoped sample and found large, antiparallel z polarization of the spin at $\bar{\Gamma}$. As shown in Fig. S11 [45], the s_z components are observed to be as large as 30%, in drastic contrast to the case of nonmagnetic TIs where $s_z = 0$ at $\bar{\Gamma}$. However, due to the limitation of the energy resolution of spin-ARPES, one cannot rule out the bulk contribution although the penetration effect predominately counts the topmost Sb-$MnBi_2Te_4$ layer at the surface [58]. Another possible scenario is that this gap does not result from the surface FM, but rather the effect of dephasing and Coulomb scattering from charged impurities, such as vacancies (Section S15 [45]) [62]. We note that such speculation simultaneously fulfills the two anomalous features of the TSS gap, i.e., remaining above T_N and increasing upon doping, but it does not perfectly fit the observed shape of the gapped bands. Other mechanisms, such as the effect of hybridization with alien d electrons from transition-metal elements [76] and lattice-distortion induced symmetry breaking [77], seem unlikely to happen here.

More evidence that exposes the underlying mechanism of the anomalous gap is thus called for.

In summary, a sizable global energy gap in the topological surface state of a magnetic topological insulator, Sb-doped $MnBi_2Te_4$, is discovered experimentally. Our systematic ARPES measurements found that this gap increases in size from near vanishing to more than 100 meV at low doping levels, but remains constant in both the low-temperature AFM and the high-temperature PM phases. The transition between the two phases is identified by the merging of two bulk conduction bands at T_N, observed both in our ARPES measurements and DFT calculations. Restoration of surface FM, weak ferromagnetism introduced by RKKY interaction, as well as the combined effect of charged impurity and quasiparticle dephasing are discussed as possible origins of the TSS gap. Remarkably, these possibilities do not hinder the topological nontriviality of the system. It is nonetheless a large, robust surface state gap with inverted band order in the bulk. Our results show unambiguously that the gap at the topological surface state of $MnBi_2Te_4$ can be tuned in a systematic way via Sb substitution. Taken collectively, we suggest that Sb-doped $MnBi_2Te_4$, comprising a single massive Dirac cone caused either by the broken $\mathcal{T}$ symmetry or the charged impurities, might be thus far the simplest material system to observe the signatures of the high-temperature axion insulator state.

We thank Prof. Xin-Cheng Xie, Haiwen Liu, Hai-Zhou Lu, Weiqiang Chen, Dr. Zhi Wang, and Dr. Wen Huang for inspiring discussions. ARPES experiments were performed with the approval of the Hiroshima Synchrotron Radiation Center (HSRC), Hiroshima, Japan under Proposals 19BG044, 19BU002, 19BU005 and 19BU012. Work at SUSTech was supported by the National Key R&D Program of China (Nos. 2020YFA0308900 and 2019YFA0704900), the National Natural Science Foundation of China (NSFC) (Nos. 12074161, 11874195, 12074163, 11804144, 11804402, and 11974156), NSFC Guangdong (No. 2016A030313650), the Guangdong Innovative and Entrepreneurial Research Team Program (Nos. 2016ZT06D348, 2017ZT07C062, and 2019ZT08C044), the Guangdong Provincial Key Laboratory of Computational Science and Material Design (No. 2019B030301001), the University Innovative Team in Guangdong Province (No. 2020KCXTD001), the Shenzhen Key Laboratory (No. ZDSYS20170303165926217), the Science, Technology and Innovation Commission of Shenzhen Municipality (Nos. KYTDPT20181011104202253 and KQTD20190929173815000), the Center for Computational Science and Engineering of SUSTech, and also with the assistance of SUSTech Core Research Facilities, especially technical support from Pico-Centre that receives support from the Presidential fund and Development and Reform Commission of Shenzhen Municipality. J.S. is supported by the SUSTech Presidential Postdoctoral Fellowship. C.C. is supported by the Shenzhen High-level Special Fund (Nos. G02206304, G02206404). Ch.L. acknowledges support from the Highlight Project (No. PHYS-HL-2020-1) of the College of Science, SUSTech.

[1] Y. Tokura, K. Yasuda, and A. Tsukazaki, Magnetic topological insulators, Nat. Rev. Phys. **1**, 126 (2019).

[2] N. P. Armitage and L. Wu, On the matter of topological insulators as magnetoelectrics, SciPost Phys. **6**, 046 (2019).

[3] P. Tang, Q. Zhou, G. Xu, and S.-C. Zhang, Dirac fermions in an antiferromagnetic semimetal, Nat. Phys. **12**, 1100 (2016).

[4] R. S. K. Mong, A. M. Essin, and J. E. Moore, Antiferromagnetic topological insulators, Phys. Rev. B **81**, 245209 (2010).

[5] J. Wang, B. Lian, X.-L. Qi, and S.-C. Zhang, Quantized topological magnetoelectric effect of the zero-plateau quantum anomalous Hall state, Phys. Rev. B **92**, 081107(R) (2015).

[6] M. Mogi, M. Kawamura, R. Yoshimi, A. Tsukazaki, Y. Kozuka, N. Shirakawa, K. S. Takahashi, M. Kawasaki, and Y. Tokura, A magnetic heterostructure of topological insulators as a candidate for an axion insulator, Nat. Mater. **16**, 516 (2017).

[7] D. Xiao, J. Jiang, J.-H. Shin, W. Wang, F. Wang, Y.-F. Zhao, C. Liu, W. Wu, M. H. W. Chan, N. Samarth, and C.-Z. Chang, Realization of the Axion Insulator State in Quantum Anomalous Hall Sandwich Heterostructures, Phys. Rev. Lett. **120**, 056801 (2018).

[8] R. Yu, W. Zhang, H.-J. Zhang, S.-C. Zhang, X. Dai, and Z. Fang, Quantized anomalous Hall effect in magnetic topological insulators, Science **329**, 61 (2010).

[9] C.-Z. Chang, J. Zhang, X. Feng, J. Shen, Z. Zhang, M. Guo, K. Li, Y. Ou, P. Wei, L.-L. Wang, Z.-Q. Ji, Y. Feng, S. Ji, X. Chen, J. Jia, X. Dai, Z. Fang, S.-C. Zhang, K. He, Y. Wang, L. Lu, X.-C. Ma, and Q.-K. Xue, Experimental observation of the quantum anomalous Hall effect in a magnetic topological insulator, Science **340**, 167 (2013).

[10] X.-L. Qi, T. L. Hughes, and S.-C. Zhang, Topological field theory of time-reversal invariant insulators, Phys. Rev. B **78**, 195424 (2008); **81**, 159901(E) (2010).

[11] L. Wu, M. Salehi, N. Koirala, J. Moon, S. Oh, and N. P. Armitage, Quantized Faraday and Kerr rotation and axion electrodynamics of a 3D topological insulator, Science **354**, 1124 (2016).

[12] D. J. E. Marsh, K. C. Fong, E. W. Lentz, L. Šmejkal, and M. N. Ali, Proposal to Detect Dark Matter using Axionic Topological Antiferromagnets, Phys. Rev. Lett. **123**, 121601 (2019).

[13] D. Zhang, M. Shi, T. Zhu, D. Xing, H. Zhang, and J. Wang, Topological Axion States in the Magnetic Insulator $MnBi_2Te_4$ with the Quantized Magnetoelectric Effect, Phys. Rev. Lett. **122**, 206401 (2019).

[14] J. Li, Y. Li, S. Du, Z. Wang, B.-L. Gu, S.-C. Zhang, K. He, W. Duan, and Y. Xu, Intrinsic magnetic topological insulators in van der Waals layered $MnBi_2Te_4$-family materials, Sci. Adv. **5**, eaaw5685 (2019).

[15] Y. Gong, J. Guo, J. Li, K. Zhu, M. Liao, X. Liu, Q. Zhang, L. Gu, L. Tang, X. Feng, D. Zhang, W. Li, C. Song, L. Wang, P. Yu, X. Chen, Y. Wang, H. Yao, W. Duan, Y. Xu, S.-C. Zhang, X. Ma, Q.-K. Xue, and K. He, Experimental realization of an intrinsic magnetic topological insulator, Chin. Phys. Lett. **36**, 076801 (2019).

[16] M. M. Otrokov, I. I. Klimovskikh, H. Bentmann, D. Estyunin, A. Zeugner, Z. S. Aliev, S. Gaß, A. U. B. Wolter, A. V. Koroleva, A. M. Shikin, M. Blanco-Rey, M. Hoffmann, I. P. Rusinov, A. Yu. Vyazovskaya, S. V. Eremeev, Yu. M. Koroteev, V. M. Kuznetsov, F. Freyse, J. Sánchez-Barriga, I. R. Amiraslanov, M. B. Babanly, N. T. Mamedov, N. A. Abdullayev, V. N. Zverev, A. Alfonsov, V. Kataev, B. Büchner, E. F. Schwier, S. Kumar, A. Kimura, L. Petaccia, G. Di Santo, R. C. Vidal, S. Schatz, K. Kißner, M. Ünzelmann, C. H. Min, Simon Moser, T. R. F. Peixoto, F. Reinert, A. Ernst, P. M. Echenique, A. Isaeva, and E. V. Chulkov, Prediction and observation of an antiferromagnetic topological insulator, Nature **576**, 416 (2019).

[17] E. D. L. Rienks, S. Wimmer, J. Sánchez-Barriga, O. Caha, P. S. Mandal, J. Růžička, A. Ney, H. Steiner, V. V. Volobuev, H. Groiss, M. Albu, G. Kothleitner, J. Michalička, S. A. Khan, J. Minár, H. Ebert, G. Bauer, F. Freyse, A. Varykhalov, O. Rader, and G. Springholz, Large magnetic gap at the Dirac point in $Bi_2Te_3/MnBi_2Te_4$ heterostructures, Nature **576**, 423 (2019).

[18] Y. Deng, Y. Yu, M. Z. Shi, Z. Guo, Z. Xu, J. Wang, X. H. Chen, and Y. Zhang, Quantum anomalous Hall effect in intrinsic magnetic topological insulator $MnBi_2Te_4$, Science **367**, 895 (2020).

[19] C. Liu, Y. Wang, H. Li, Y. Wu, Y. Li, J. Li, K. He, Y. Xu, J. Zhang, and Y. Wang, Robust axion insulator and Chern insulator phases in a two-dimensional antiferromagnetic topological insulator, Nat. Mater. **19**, 522 (2020).

[20] T. Hirahara, S. V. Eremeev, T. Shirasawa, Y. Okuyama, T. Kubo, R. Nakanishi, R. Akiyama, A. Takayama, T. Hajiri, S.-I. Ideta, M. Matsunami, K. Sumida, K. Miyamoto, Y. Takagi, K. Tanaka, T. Okuda, T. Yokoyama, S.-I. Kimura, S. Hasegawa, and E. V. Chulkov, Large-gap magnetic topological heterostructure formed by subsurface incorporation of a ferromagnetic layer, Nano Lett. **17**, 3493 (2017).

[21] K. G. S. Ranmohotti, H. Djieutedjeu, and P. F. P. Poudeu, Chemical manipulation of magnetic ordering in $Mn_{1-x}Sn_xBi_2Se_4$ solid-solutions, J Am. Chem. Soc. **134**, 14033 (2012).

[22] J. Wu, F. Liu, M. Sasase, K. Ienaga, Y. Obata, R. Yukawa, K. Horiba, H. Kumigashira, S. Okuma, T. Inoshita, and H. Hosono, Natural van der Waals heterostructural single crystals with both magnetic and topological properties, Sci. Adv. **5**, eaax9989 (2019).

[23] M. Z. Shi, B. Lei, C. S. Zhu, D. H. Ma, J. H. Cui, Z. L. Sun, J. J. Ying, and X. H. Chen, Magnetic and transport properties in the magnetic topological insulators $MnBi_2Te_4(Bi_2Te_3)_n$ ($n = 1, 2$), Phys. Rev. B **100**, 155144 (2019).

[24] J.-Q. Yan, Q. Zhang, T. Heitmann, Z. Huang, K. Y. Chen, J.-G. Cheng, W. Wu, D. Vaknin, B. C. Sales, and R. J. McQueeney, Crystal growth and magnetic structure of $MnBi_2Te_4$, Phys. Rev. Mater. **3**, 064202 (2019).

[25] A. Zeugner, F. Nietschke, A. U. B. Wolter, S. Gaß, R. C. Vidal, T. R. F. Peixoto, D. Pohl, C. Damm, A. Lubk, R. Hentrich, S. K. Moser, C. Fornari, C. H. Min, S. Schatz, K. Kißner, M. Ünzelmann, M. Kaiser, F. Scaravaggi, B. Rellinghaus, K. Nielsch, C. Hess, B. Büchner, F. Reinert, H. Bentmann, O. Oeckler, T. Doert, M. Ruck, and A. Isaeva, Chemical aspects of the candidate antiferromagnetic topological insulator $MnBi_2Te_4$, Chem. Mater. **31**, 2795 (2019).

[26] L. Ding, C. Hu, F. Ye, E. Feng, N. Ni, and H. Cao, Crystal and magnetic structures of magnetic topological insulators $MnBi_2Te_4$ and $MnBi_4Te_7$, Phys. Rev. B **101**, 020412(R) (2020).

[27] C. Hu, L. Ding, K. N. Gordon, B. Ghosh, H.-J. Tien, H. Li, A. G. Linn, S.-W. Lien, C.-Y. Huang, S. Mackey, J. Liu, P. V. S. Reddy, B. Singh, A. Agarwal, A. Bansil, M. Song, D. Li, S.-Y. Xu, H. Lin, H. Cao, T.-R. Chang, D. Dessau, and N. Ni, Realization of an intrinsic ferromagnetic topological state in $MnBi_8Te_{13}$, Sci. Adv. **6**, eaba4275 (2020).

[28] C. Hu, K. N. Gordon, P. Liu, J. Liu, X. Zhou, P. Hao, D. Narayan, E. Emmanouilidou, H. Sun, Y. Liu, H. Brawer, A. P. Ramirez, L. Ding, H. Cao, Q. Liu, D. Dessau, and N. Ni, A van der Waals antiferromagnetic topological insulator with weak interlayer magnetic coupling, Nat. Commun. **11**, 97 (2020).

[29] Y.-J. Hao, P. Liu, Y. Feng, X.-M. Ma, E. F. Schwier, M. Arita, S. Kumar, C. Hu, R. Lu, M. Zeng, Y. Wang, Z. Hao, H.-Y. Sun, K. Zhang, J. Mei, N. Ni, L. Wu, K. Shimada, C. Chen, Q. Liu, and C. Liu, Gapless Surface Dirac Cone in Antiferromagnetic Topological Insulator $MnBi_2Te_4$, Phys. Rev. X **9**, 041038 (2019).

[30] H. Li, S.-Y. Gao, S.-F. Duan, Y.-F. Xu, K.-J. Zhu, S.-J. Tian, J.-C. Gao, W.-H. Fan, Z.-C. Rao, J.-R. Huang, J.-J. Li, D.-Y. Yan, Z.-T. Liu, W.-L. Liu, Y.-B. Huang, Y.-L. Li, Y. Liu, G.-B. Zhang, P. Zhang, T. Kondo, S. Shin, H.-C. Lei, Y.-G. Shi, W.-T. Zhang, H.-M. Weng, T. Qian, and H. Ding, Dirac Surface States in Intrinsic Magnetic Topological Insulators $EuSn_2As_2$ and $MnBi_{2n}Te_{3n+1}$, Phys. Rev. X **9**, 041039 (2019).

[31] Y. J. Chen, L. X. Xu, J. H. Li, Y. W. Li, H. Y. Wang, C. F. Zhang, H. Li, Y. Wu, A. J. Liang, C. Chen, S. W. Jung, C. Cacho, Y. H. Mao, S. Liu, M. X. Wang, Y. F. Guo, Y. Xu, Z. K. Liu, L. X. Yang, and Y. L. Chen, Topological electronic structure and its temperature evolution in antiferromagnetic topological insulator $MnBi_2Te_4$, Phys. Rev. X **9**, 041040 (2019).

[32] B. Chen, F. Fei, D. Zhang, B. Zhang, W. Liu, S. Zhang, P. Wang, B. Wei, Y. Zhang, Z. Zuo, J. Guo, Q. Liu, Z. Wang, X. Wu, J. Zong, X. Xie, W. Chen, Z. Sun, S. Wang, Y. Zhang, M. Zhang, X. Wang, F. Song, H. Zhang, D. Shen, and B. Wang, Intrinsic magnetic topological insulator phases in the Sb doped $MnBi_2Te_4$ bulks and thin flakes, Nat. Commun. **10**, 4469 (2019).

[33] Y. Hu, L. Xu, M. Shi, A. Luo, S. Peng, Z. Y. Wang, J. J. Ying, T. Wu, Z. K. Liu, C. F. Zhang, Y. L. Chen, G. Xu, X.-H. Chen, and J.-F. He, Universal gapless Dirac cone and tunable topological states in $(MnBi_2Te_4)_m(Bi_2Te_3)_n$ heterostructures, Phys. Rev. B **101**, 161113(R) (2020).

[34] P. Swatek, Y. Wu, L.-L. Wang, K. Lee, B. Schrunk, J.-Q. Yan, and A. Kaminski, Gapless Dirac surface states in the antiferromagnetic topological insulator $MnBi_2Te_4$, Phys. Rev. B **101**, 161109(R) (2020).

[35] N. H. Jo, L.-L. Wang, R.-J. Slager, J. Yan, Y. Wu, K. Lee, B. Schrunk, A. Vishwanath, and A. Kaminski, Intrinsic axion insulating behavior in antiferromagnetic $MnBi_6Te_{10}$, Phys. Rev. B **102**, 045130 (2020).

[36] X.-M. Ma, Z. Chen, E. F. Schwier, Y. Zhang, Y.-J. Hao, S. Kumar, R. Lu, J. Shao, Y. Jin, M. Zeng, X.-R. Liu, Z. Hao, K. Zhang, W. Mansuer, C. Song, Y. Wang, B. Zhao, C. Liu, K. Deng, J. Mei, K. Shimada, Y. Zhao, X. Zhou, B. Shen, W. Huang, C. Liu, H. Xu, and C. Chen, Hybridization-induced gapped and gapless states on the surface of magnetic topological insulators, Phys. Rev. B **102**, 245136 (2020).

[37] X. Wu, J. Li, X.-M. Ma, Y. Zhang, Y. Liu, C.-S. Zhou, J. Shao, Q. Wang, Y.-J. Hao, Y. Feng, E. F. Schwier, S. Kumar, H. Sun, P. Liu, K. Shimada, K. Miyamoto, T. Okuda, K. Wang, M. Xie, C. Chen, Q. Liu, C. Liu, and Y. Zhao, Distinct Topological Surface

States on the Two Terminations of $MnBi_4Te_7$, Phys. Rev. X **10**, 031013 (2020).

[38] K. N. Gordon, H. Sun, C. Hu, A. G. Linn, H. Li, Y. Liu, P. Liu, S. Mackey, Q. Liu, N. Ni, and D. Dessau, Strongly gapped topological surface states on protected surfaces of antiferromagnetic $MnBi_4Te_7$ and $MnBi_6Te_{10}$, arXiv:1910.13943 (2019).

[39] R. C. Vidal, H. Bentmann, T. R. F. Peixoto, A. Zeugner, S. Moser, C.-H. Min, S. Schatz, K. Kißner, M. Ünzelmann, C. I. Fornari, H. B. Vasili, M. Valvidares, K. Sakamoto, D. Mondal, J. Fujii, I. Vobornik, S. Jung, C. Cacho, T. K. Kim, R. J. Koch, C. Jozwiak, A. Bostwick, J. D. Denlinger, E. Rotenberg, J. Buck, M. Hoesch, F. Diekmann, S. Rohlf, M. Kalläne, K. Rossnagel, M. M. Otrokov, E. V. Chulkov, M. Ruck, A. Isaeva, and F. Reinert, Surface states and Rashba-type spin polarization in antiferromagnetic $MnBi_2Te_4(0001)$, Phys. Rev. B **100**, 121104(R) (2019).

[40] R. C. Vidal, A. Zeugner, J. I. Facio, R. Ray, M. H. Haghighi, A. U. B. Wolter, L. T. C. Bohorquez, F. Caglieris, S. Moser, T. Figgemeier, T. R. F. Peixoto, H. B. Vasili, M. Valvidares, S. Jung, C. Cacho, A. Alfonsov, K. Mehlawat, V. Kataev, C. Hess, M. Richter, B. Büchner, J. van den Brink, M. Ruck, F. Reinert, H. Bentmann, and A. Isaeva, Topological Electronic Structure and Intrinsic Magnetization in $MnBi_4Te_7$: A Bi_2Te_3 Derivative with a Periodic Mn Sublattice, Phys. Rev. X **9**, 041065 (2019).

[41] W. Ko, M. Kolmer, J. Yan, A. D. Pham, M. Fu, F. Lüpke, S. Okamoto, Z. Gai, P. Ganesh, and A.-P. Li, Realizing gapped surface states in the magnetic topological insulator $MnBi_{2-x}Sb_xTe_4$, Phys. Rev. B **102**, 115402 (2020).

[42] D. O. Scanlon, P. D. King, R. P. Singh, A. de la Torre, S. M. Walker, G. Balakrishnan, F. Baumberger, and C. R. Catlow, Controlling bulk conductivity in topological insulators: Key role of anti-site defects, Adv. Mater. **24**, 2154 (2012).

[43] J. Zhang, C.-Z. Chang, Z. Zhang, J. Wen, X. Feng, K. Li, M. Liu, K. He, L. Wang, X. Chen, Q.-K. Xue, X. Ma, and Y. Wang, Band structure engineering in $(Bi_{1-x}Sb_x)_2Te_3$ ternary topological insulators, Nat. Commun. **2**, 574 (2011).

[44] M. Neupane, S.-Y. Xu, L. A. Wray, A. Petersen, R. Shankar, N. Alidoust, C. Liu, A. Fedorov, H. Ji, J. M. Allred, Y. S. Hor, T.-R. Chang, H.-T. Jeng, H. Lin, A. Bansil, R. J. Cava, and M. Z. Hasan, Topological surface states and Dirac point tuning in ternary topological insulators, Phys. Rev. B **85**, 235406 (2012).

[45] See Supplemental Information at http://link.aps.org/supplemental/10.1103/PhysRevB.103.L121112 for Methods, Sections S1-S15 and Figures S1-S14. References [30,32,46–64] are included.

[46] Z. S. Aliev, I. R. Amiraslanov, D. I. Nasonova, A. V. Shevelkov, N. A. Abdullayev, Z. A. Jahangirli, E. N. Orujlu, M. M. Otrokov, N. T. Mamedov, M. B. Babanly, and E. V. Chulkov, Novel ternary layered manganese bismuth tellurides of the MnTe-Bi_2Te_3 system: Synthesis and crystal structure, J. Alloys Compd. **789**, 443 (2019).

[47] T. Okuda, K. Miyamoto, A. Kimura, H. Namatame, and M. Taniguchi, A double VLEED spin detector for high-resolution three dimensional spin vectorial analysis of anisotropic Rashba spin splitting, J Elec. Spec. Rel. Phenom. **201**, 23 (2015).

[48] G. Kresse and J. Furthmüller, Efficient iterative schemes for *ab initio* total-energy calculations using a plane-wave basis set, Phys. Rev. B **54**, 11169 (1996).

[49] J. P. Perdew, K. Burke, and M. Ernzerhof, Generalized Gradient Approximation Made Simple, Phys. Rev. Lett. **77**, 3865 (1996).

[50] V. I. Anisimov, J. Zaanen, and O. K. Andersen, Band theory and Mott insulators: Hubbard *U* instead of Stoner *I*, Phys. Rev. B **44**, 943 (1991).

[51] G. Kresse and D. Joubert, From ultrasoft pseudopotentials to the projector augmented-wave method, Phys. Rev. B **59**, 1758 (1999).

[52] T. B. Boykin, N. Kharche, G. Klimeck, and M. Korkusinski, Approximate bandstructures of semiconductor alloys from tight-binding supercell calculations, J. Phys.: Condens. Matter **19**, 036203 (2007).

[53] T. B. Boykin and G. Klimeck, Practical application of zone-folding concepts in tight-binding calculations, Phys. Rev. B **71**, 115215 (2005).

[54] P. V. C. Medeiros, S. Stafström, and J. Björk, Effects of extrinsic and intrinsic perturbations on the electronic structure of graphene: Retaining an effective primitive cell band structure by band unfolding, Phys. Rev. B **89**, 041407(R) (2014).

[55] P. V. C. Medeiros, S. S. Tsirkin, S. Stafström, and J. Björk, Unfolding spinor wave functions and expectation values of general operators: Introducing the unfolding-density operator, Phys. Rev. B **91**, 041116(R) (2015).

[56] S.-Y. Xu, M. Neupane, C. Liu, D. Zhang, A. Richardella, L. A. Wray, N. Alidoust, M. Leandersson, T. Balasubramanian, J. Sánchez-Barriga, O. Rader, G. Landolt, B. Slomski, J. H. Dil, J. Osterwalder, T.-R. Chang, H.-T. Jeng, H. Lin, A. Bansil, N. Samarth, and M. Z. Hasan, Hedgehog spin texture and Berry's phase tuning in a magnetic topological insulator, Nat. Phys. **8**, 616 (2012).

[57] J. Sánchez-Barriga, A. Varykhalov, J. Braun, S.-Y. Xu, N. Alidoust, O. Kornilov, J. Minár, K. Hummer, G. Springholz, G. Bauer, R. Schumann, L. V. Yashina, H. Ebert, M. Z. Hasan, and O. Rader, Photoemission of Bi_2Se_3 with Circularly Polarized Light: Probe of Spin Polarization or Means for Spin Manipulation? Phys. Rev. X **4**, 011046 (2014).

[58] X. Zhang, Q. Liu, J.-W. Luo, A. J. Freeman, and A. Zunger, Hidden spin polarization in inversion-symmetric bulk crystals, Nat. Phys. **10**, 387 (2014).

[59] T. Sato, K. Segawa, K. Kosaka, S. Souma, K. Nakayama, K. Eto, T. Minami, Y. Ando, and T. Takahashi, Unexpected mass acquisition of Dirac fermions at the quantum phase transition of a topological insulator, Nat. Phys. **7**, 840 (2011).

[60] J. Sánchez-Barriga, A. Varykhalov, G. Springholz, H. Steiner, R. Kirchschlager, G. Bauer, O. Caha, E. Schierle, E. Weschke, A. A. Ünal, S. Valencia, M. Dunst, J. Braun, H. Ebert, J. Minár, E. Golias, L. V. Yashina, A. Ney, V. Holý, and O. Rader, Nonmagnetic band gap at the Dirac point of the magnetic topological insulator $(Bi_{1-x}Mn_x)_2Se_3$, Nat. Commun. **7**, 10559 (2016).

[61] T. Yilmaz, A. Pertsova, W. Hines, E. Vescovo, K. Kaznatcheev, A. V. Balatsky, and B. Sinkovic, Gap-like feature observed in the non-magnetic topological insulators, J Phys. Condens. Matter **32**, 145503 (2020).

[62] H. Liu, H. Jiang, Q. F. Sun, and X. C. Xie, Dephasing Effect on Backscattering of Helical Surface States in 3D Topological Insulators, Phys. Rev. Lett. **113**, 046805 (2014).

[63] F. Delgado and J. Fernández-Rossier, Spin decoherence of magnetic atoms on surfaces, Prog. Surf. Sci. **92**, 40 (2017).

[64] L. Bellaiche and D. Vanderbilt, Virtual crystal approximation revisited: Application to dielectric and piezoelectric properties of perovskites, Phys. Rev. B **61**, 7877 (2000).

[65] S. V. Eremeev, M. M. Otrokov, and E. V. Chulkov, Competing rhombohedral and monoclinic crystal structures in $MnPn_2Ch_4$ compounds: An *ab-initio* study, J Alloys Compd. **709**, 172 (2017).

[66] J. Q. Yan, S. Okamoto, M. A. McGuire, A. F. May, R. J. McQueeney, and B. C. Sales, Evolution of structural, magnetic, and transport properties in $MnBi_{2-x}Sb_xTe_4$, Phys. Rev. B **100**, 104409 (2019).

[67] L. Zhou, Z. Tan, D. Yan, Z. Fang, Y. Shi, and H. Weng, Topological phase transition in the layered magnetic compound $MnSb_2Te_4$: Spin-orbit coupling and interlayer coupling dependence, Phys. Rev. B **102**, 085114 (2020).

[68] Y. Chen, Y.-W. Chuang, S. H. Lee, Y. Zhu, K. Honz, Y. Guan, Y. Wang, K. Wang, Z. Mao, J. Zhu, C. Heikes, P. Quarterman, P. Zajdel, J. A. Borchers, and W. Ratcliff, II, Ferromagnetism in van der Waals compound $MnSb_{1.8}Bi_{0.2}Te_4$, Phys. Rev. Mater. **4**, 064411 (2020).

[69] M. H. Du, J. Yan, V. R. Cooper, and M. Eisenbach, Tuning Fermi levels in intrinsic antiferromagnetic topological insulators $MnBi_2Te_4$ and $MnBi_4Te_7$ by defect engineering and chemical doping, Adv. Funct. Mater. **31**, 2006516 (2021).

[70] A. Zunger, S.-H. Wei, L. G. Ferreira, and J. E. Bernard, Special Quasirandom Structures, Phys. Rev. Lett. **65**, 353 (1990).

[71] T_N is found to decrease monotonically with increasing x, from 23.89 K for $x = 0$ (S1) to ~23 K for $x_{\text{nominal}} = 0.1$ (S5).

[72] Note that a nonvanishing TSS gap is found on the undoped sample from our multipeak fitting procedure (Fig. S6). This gap is much smaller than what the DFT calculation predicts (~80 meV). Such behavior is consistent with the near gapless feature found by ARPES in Refs. [29–32,34], among which Ref. [30] pointed out specifically the existence of a gap of about 10 meV.

[73] Note that previous ARPES studies on Sb-$MnBi_2Te_4$ observe a continuous p-doping behavior with increasing x values and an n-p transition at $x \sim 0.3$ [32]; evidence of a sizable gap at $x = 0.32$ (where the system is p-typed) is provided by studying the quasiparticle interference pattern [41], but no momentum-resolved information is available prior to this work on how the surface and the bulk gaps evolve either with x or with temperature.

[74] T. Murakami, Y. Nambu, T. Koretsune, X. Gu, T. Yamamoto, C. M. Brown, and H. Kageyama, Realization of interlayer ferromagnetic interaction in $MnSb_2Te_4$ toward the magnetic Weyl semimetal state, Phys. Rev. B **100**, 195103 (2019).

[75] Q. Liu, C.-X. Liu, C. Xu, X.-L. Qi, and S.-C. Zhang, Magnetic Impurities on the Surface of a Topological Insulator, Phys. Rev. Lett. **102**, 156603 (2009).

[76] A. Polyakov, C. Tusche, M. Ellguth, E. D. Crozier, K. Mohseni, M. M. Otrokov, X. Zubizarreta, M. G. Vergniory, M. Geilhufe, E. V. Chulkov, A. Ernst, H. L. Meyerheim, and S. S. P. Parkin, Instability of the topological surface state in Bi_2Se_3 upon deposition of gold, Phys. Rev. B **95**, 180202(R) (2017).

[77] P. S. Mandal, G. Springholz, V. V. Volobuev, O. Caha, A. Varykhalov, E. Golias, G. Bauer, O. Rader, and J. Sánchez-Barriga, Topological quantum phase transition from mirror to time reversal symmetry protected topological insulator, Nat. Commun. **8**, 968 (2017).